Typha latifolia and *Thelypteris palustris* behavior in a pilot system for the refinement of livestock wastewaters: a case of study

Nadia Stroppa[a], Elisabetta Onelli[a], Monika Hejna[b], Luciana Rossi[b], Assunta Gagliardi[c], Luca Bini[d], Antonella Baldi[b] and Alessandra Moscatelli[a§]

[a] Department of Biosciences, University of Milano, Via Celoria 26, 20133 Milan (Italy)

[b] Department of Health, Animal Science and Food Safety, University of Milano, Via Celoria 10, 20133 Milan (Italy)

[c] Dipartimento di Biologia Cellulare, Computazionale e Integrata - CIBIO, University of Trento, Via Sommarive 9, Povo 38123 Trento (Italy)

[d] Department of Life Science, University of Siena, Via Aldo Moro 2, 53100 Siena (Italy)

[§] **Corresponding author**: Alessandra Moscatelli, Department of Biosciences, University of Milano, Via Celoria 26, 20133 Milan (Italy); alessandra.moscatelli@unimi.it; Phone number: 0039-02-50314846

Author e-mail:

Nadia Stroppa: nadia.stroppa@unimi.it

Elisabetta Onelli: elisabetta.onelli@unimi.it

Monika Hejna: monika.hejna@unimi.it

Luciana Rossi: Luciana.rossi@unimi.it

Assunta Gagliardi: assunta.gagliardi@unitn.it

Luca Bini: luca.bini@unisi.it

Antonella Baldi: antonella.baldi@unimi.it

Alessandra Moscatelli: alessandra.moscatelli@unimi.it

Highlights:

- *Thelypteris palustris* was more affected by metals than *Typha latifolia*.
- Salts of Zn and Cu induced cell wall remodeling and carbohydrate metabolism changes in both plants.
- Similar morphological alterations were induced by different mechanisms in both plants.

ABSTRACT

In animal livestock heavy metals are widely used as feed additives to control enteric bacterial infections as well as to enhance the integrity of the immune system. As these metals are only partially adsorbed by animals, the content of heavy metals in manure and wastewaters causes soil and ground water contamination, with Zn^{2+} and Cu^{2+} being the most critical output from pig livestock.

Phytoremediation is considered a valid strategy to improve the purity of wastewaters. This work studied the effect of Zn^{2+} and Cu^{2+} on the morphology and protein expression in *Thelypteris palustris* and *Typha latifolia* plants, cultured in a wetland pilot system.

Despite the absence of macroscopic alterations, remodeling of cell walls and changes in carbohydrate metabolism were observed in the rhizomes of both plants and in leaves of *Thelypteris palustris*. However, similar modifications seemed to be determined by the alterations of different mechanisms in these plants. These data also suggested that marsh ferns are more sensitive to metals than monocots. Whereas toleration mechanisms seemed to be activated in *Typha latifolia*, in *Thelypteris palustris* the observed modifications appeared as slight toxic effects due to metal exposure.

This study clearly indicates that both plants could be successfully employed in *in situ* phytoremediation systems, to remove Cu^{2+} and Zn^{2+} at concentrations that are ten times higher than the legal limits, without affecting plant growth.

Keywords: *Typha latifolia*, *Thelypteris palustris*, phytodepuration, livestock wastewaters, heavy metals

1. INTRODUCTION

Livestock wastewaters are usually reused in agriculture after traditional depuration treatment (Nicholson et al. 2003). However, these wastewaters often contain metals that should be removed to prevent field contamination. The presence of metals is related to the animals' diet, which is enriched with this type of essential compounds to enhance the integrity of the immune system (Liu et al. 2018, Reg. UE1831/2003). Phytodepuration is a low cost and ecologically friendly technology for civil and industrial wastewater refinement (Peterson, 1998). It also improves livestock wastewaters in terms of organic substances through the construction of wetlands (Anning et al., 2013; Yang and Ye, 2009). However, its application in terms of metal removal from livestock wastewaters is still scarcely documented (Almeida et al., 2016).

In order to improve the knowledge regarding the efficiency and applicability of phytodepuration for metal removal from animal wastewaters, we set up two types of mesocosms, with *Typha latifolia* or *Thelypteris palustris* (marsh fern) to treat water spiked and not spiked with Zn^{2+} (44.02 mg/L) and Cu^{2+} (8.63 mg/L), the main metals present in livestock wastewaters. Chemical analyses showed that both plants were tolerant (they did not show any macroscopic alteration) and accumulated substantial amounts of metals in their tissues, particularly in the aboveground organs (see accompanying paper, Hejna et al., 2019). In particular, treated *T. latifolia* began to accumulate Zn^{2+} and Cu^{2+} after 15 days of metal exposure, since there was only a significant increase in metal concentration in T2 (Zn: $p < 0.001$; TLT = 271.64±17.71 vs. TLC = 55.79±17.71 mg/kg; Cu: $p < 0.001$; TLT =47.54±3.56 vs. TLC =15.20±3.56 mg/kg), suggesting that *T. latifolia* can accumulate Zn^{2+} and Cu^{2+} in its organs 45 days after the treatment. Moreover, *T. palustris* were also able to accumulate Zn^{2+} and Cu^{2+} in their organs. In fact, higher concentrations of metals were detected

in TPT than in the control already 15 days (T1) after metal addition (Zn: $p < 0.001$; TPT = 414.67±17.71 vs. TPC = 85.62±17.71 mg/kg; Cu: $p < 0.001$; TPT = 136.12±3.56 vs. TPC = 18.25±3.56 mg/kg). Furthermore, we observed the decreasing trend of Zn and Cu in water and soil in treated mesocosms (TLT, TPT) in the end of the experiment (T2) compared with T0 for *T. latifolia* and *T. plaustris* plants (see accompayning paper Hejna et al. 2019).

However, the marsh fern was more efficient than *T. latifolia*, accumulating higher concentrations of all the metals in its organs more quickly. However, the mechanisms behind the tolerance and metal uptake in *T. latifolia* and *T. palustris* are not well known, despite their importance in understanding how systems work and thus how to maintain/increase their efficiency.

Plants growing in heavy metal polluted environments employ several mechanisms to increase stress tolerance or to prevent the entry of metals into the cells. Stress tolerance involves biochemical processes through the action of chaperone proteins, glutathione, metallothioneins, and phytochelatins (Doğanlar, 2013; Hasan et al, 2017; Petraglia et al., 2014; Yadav 2010). In various plants, several genes induced under metal stress have been identified (Dubey et al., 2014; Kumar and Trivedi, 2016; Singh et al., 2016; Tiwari and Lata, 2018). Transcription factors or other proteins involved in metal detoxification, signal transduction, stress signal, ROS signaling have been identified as having an important role in heavy metal tolerance (Collin et al, 2008; Lingua et al., 2012; Rao et al., 2011; Viehweger 2014).

On the other hand, mechanisms of stress avoidance act by limiting the metal assimilation by the root through the modification of the rhizosphere (Małachowska-Jutsz and Gnida 2015; Meier et al., 2012), binding metals in the cell wall (Colzi et al., 2012; Krzesłowska 2011; Le Gall et al., 2015; Oves et al., 2016), removing metals by glands and hydathodes or accumulating metals in vacuoles of ageing leaves (Małachowska-Jutsz and Gnida 2015).

These tolerance mechanisms have also been reported in wetland plants which were shown to synthesize phytochelatins, peptides and exudates to chelate-free metal ions, to increase

antioxidant enzyme activities and sequester heavy metals in organs or subcellular compartments (Fediuc and Erdei, 2002; Higuchi et al., 2015, Yang and Ye, 2009; Yang et al., 2000).

The aim of this work was to investigate the mechanisms behind the capacity of *T. latifolia* and *T. palustris* to accumulate Zn^{2+} and Cu^{2+} by analyzing the proteome and the morphology of cells and tissues in plants grown in a pilot wetland system.

Microscopy and proteomic analyses were performed on the leaves and rhizomes of plants after 45 days of metal exposure. For microscopical observations, sections were obtained from three different plants grown with or without the mineral feed additive premix, containing Zn^{2+} and Cu^{2+} at a concentration 14 times higher than the legal limit. Treatment was performed at single concentration of metals in order to observe phytoremediation in realistic farm condition. Morphological changes were observed in the rhizomes of both plants and in leaves of *T. palustris*, suggesting cell wall remodeling and changes in the carbohydrate metabolism. Interestingly, modifications were similar in the two plant species, however they seemed to be determined by different mechanisms. The morphological changes in treated plants were more pronounced in *T. palustris* than *T. latifolia*, thus revealing their higher sensitivity to heavy metals. Regarding proteomes, no modification was observed in *T. palustris*, while few changes were observed in the 1D-gel electrophoresis protein profile of *T. latifolia*, partially explaining the morphological modifications observed by light and TEM microscopy.

2. MATERIALS AND METHODS

2.1 Plant culture and sampling

A pilot wetland system comprising 4 tanks (2 m x 2 m x 1.2 m) was prepared in the Botanical Gardens of Milan University. Tanks were first lined with waterproof cloths, and two layers of stone chippings (diameter 1-3 cm and 1 cm) and sand were put in each tank. This substratum became sediment upon the addition of water. Finally, 210 kg of loam for plant culture (Flox Containerpflanzen, Blumenerde VitaFlor) was layered on the substratum. The same quantity

130 of tap water (650 L) was added to each tank before placing the plants (purchased from Centro
131 Flora Autoctona, Galbiate, LC, Italy).
132 Three-month-old plants of *T. latifolia* (30/tank) were placed in two tanks together with
133 plants of *T. palustris* (60/tank). After 15 days (T0), in two tanks (metals: Met), one containing *T.*
134 *latifolia* and the second containing *T. palustris*, the water was contaminated with Cu^{2+} and Zn^{2+} at
135 8.63 mg/L and 44.02 mg/L final concentrations, by dissolving 1.5 Kg of the mineral feed additive
136 premix (feed Maxi CRC 0.5% supplied by Alpha). The water in the other two tanks (controls: Co)
137 was not modified.
138 Three plants were sampled in each of the four tanks after the premix addition (T0) and 45
139 days (T2) after the plants had been placed. Before sampling each tank was divided into three
140 regions and one plant was sampled from each region.
141
142 **2.2 Light and transmission electron microscopy**
143 Aerial (leaves) and subaerial (rhizomes/roots) organs of *T. latifolia* (Co/Met) and *T.*
144 *palustris* (Co/Met) taken at different times were incubated in fixing solution (0.04 M Cacodylate
145 pH 6.9, 2% Formaldehyde, 2% Glutaraldehyde) overnight at room temperature. Samples were
146 repeatedly rinsed in 0.04 M Cacodylate pH 6.9, dehydrated with increasing concentrations of
147 ethanol and embedded in LR white resin (Sigma). Semi-fine sections (2 μm) and ultra-thin sections
148 (80 nm), were obtained using a Reichert Jung Ultracut E microtome.
149 The semi-fine sections were stained by 1% toluidine blue or Lugol and observed with a
150 Leica DMRB light microscope. Ultra-thin sections were stained with 3% uranyl-acetate and
151 observed with an EFTEM LEO 912AB transmission electron microscope (Zeiss) working at 80
152 kV.
153 Plants were collected from different corners of the wetland system and, in order to observe
154 rhizomes at the same developmental stage, rhizomes with a comparable diameter were collected,
155 located at the same distance from the shoots.

2.3 Indirect immunofluorescence and confocal microscopy

Rhizome sections of *T. latifolia* and *T. palustris* were put on slides and allowed to rehydrate by incubating them with 1% BSA (bovine serum albumin) in TBS (Tris/HCl 0.05M pH 7.5, NaCl 0.15M), in a moist chamber at room temperature for 45 minutes. Sections were rinsed once with TBS, and then incubated with LM19 and JIM7, the antibodies against low esterified (LEPs) and high esterified pectins (HEPs), respectively (PlantProbes). Both primary antibodies were diluted 1:10 and the incubation was performed overnight at 4°C. Sections were rinsed twice in TBS and then incubated with the secondary antibody FITC conjugated (Rabbit Anti-Rat IgG+IgM+IgA H&L; Abcam) for two hours at room temperature in the dark. Control experiments were also performed, in which the primary antibody was omitted.

Samples were observed using a Leica TCS NT SP2 confocal microscope; a 20X lens (zoom 2) was used for imaging. The 488-nm laser line was used to excite FITC and the fluorescence was collected in the emission window 494–550 nm. The organs of at least three plants for each tank were analyzed.

2.4 Protein extraction

Leaves and rhizomes of *T. latifolia* and *T. palustris* were frozen in liquid nitrogen immediately after collection and stored at -80°C. Leaves and rhizomes were homogenized in liquid nitrogen and nitrogen ground powder was resuspended in five volumes of precooled precipitation solution (10% TCA and 20 mM DTT in acetone). Proteins were precipitated overnight at -20°C, then washed twice for 1 h at -20°C with 20 mM DTT in acetone and pelleted by centrifugation for 30 minutes at 26000 x g at 4°C. Pellets were dried for 10 minutes under vacuum and resuspended in LSB1X for 1D-gel electrophoresis. Samples were sonicated for 30 minutes in a water-bath sonicator at 20°C. The extracts were centrifuged for 30 minutes at 26000 x g, at 15°C and the supernatants were collected and stored at -80°C.

182 Protein concentration was determined by the Bradford protein assay (Bradford, 1976).

183

184 **2.5 One-dimensional electrophoresis**

185 Proteins were resolved in denaturing 10% acrylamide 1D-gels in a discontinuous buffer
186 system (Laemmli, 1970). MiniVe Vertical Electrophoresis System (GE Healthcare, USA) was
187 used for analytical one-dimensional electrophoresis. For the preparatory 1D-gel electrophoresis of
188 *T. latifolia* rhizomes, polypeptides were separated using 17 cm x 20 cm, 1.5 mm thick gels
189 (Elettrofor, Rovigo, Italy). Proteins were visualized with Coomassie brilliant blue R250 and silver
190 staining (Sinha et al., 2001). Three replicas were analyzed for at least three plants per tank.

191

192 **2.6 Mass spectrometry and protein identification**

193 Protein identification was performed as previously described (Hellman et al., 1995; Soskic
194 et al., 1999). Bands of interest were manually excised, destained in ammonium bicarbonate 2.5
195 mM and acetonitrile 50% (v/v), and acetonitrile dehydrated. Before protein digestion, 1D gel-
196 resolved proteins were reduced with 10 mM DTE in 25 mM ammonium bicarbonate (1 h at 56˚C)
197 and then alkylated with 55 mM iodoacetamide in 25 mM ammonium bicarbonate at room
198 temperature (45 min, in darkness). After incubation with 50 mM ammonium bicarbonate (10 min),
199 protein bands were acetonitrile dehydrated. 1D gel-resolved proteins were rehydrated in trypsin
200 solution (Sigma Aldrich, Italy) and in-gel protein digestion was performed by an overnight
201 incubation at 37˚C. For MALDI-TOF MS, 0.75 ml of each protein digest was directly spotted onto
202 the MALDI target and air-dried. A total of 0.75 ml of an alpha-cyano-4-hydroxycynnamic acid
203 matrix solution was added to the dried samples and allowed to dry again. Mass spectra were
204 acquired using an Ultraflex III MALDI-TOF/TOF mass spectrometer (Bruker Daltonics, Billerica,
205 MA, United States). Spectra were analyzed by Flex Analysis v. 3.0. Peptide mass fingerprinting
206 (PMF) database searches was carried out in NCBInr or Swiss-Prot/TrEMBL databases set for
207 Viridiplantae (Green Plants) using Mascot (Matrix Science Ltd., London, UK,

208 http://www.matrixscience. com) with the following settings: experimental and theoretical PMF
209 patterns with a Dmass less than 100 ppm, trypsin as the digestion enzyme, one allowed missed
210 cleavage, carbamidomethylation of cysteine as a fixed modification, and oxidation of methionine
211 as a variable modification. The parameters used to accept identifications were the number of
212 matched peptides, extent of sequence coverage, and probabilistic score. Only peptides with
213 individual ion scores of $p < 0.05$ were significant.
214
215 **3. RESULTS**
216 **3.1 Morphological changes induced by metals are revealed by light and transmission electron**
217 **microscopy in leaves of *T. palustris* and *T. latifolia***
218 *Thelypteris palustris* and *T. latifolia*, grown in the wetland apparatus tanks prepared as
219 previously described, did not show alterations in macroscopical morphology and no differences
220 were observed between control and treated plants. New leaves were produced by plants and no
221 discoloration or chlorosis, due to photosynthetic activity alteration, was observed (Fig. S1; see
222 Supplementary material). In addition, by rhizome expansion *T. latifolia* plants were able to
223 vegetatively reproduce.
224 Plant exposure to metals induces cell responses which involve metabolism modifications
225 and morphology remodeling (Arif et al, 2016; Molas et al, 2002; Oves et al, 2016; Sandalio et al.
226 2001; Todeschini et al. 2011). To reveal the morphological changes, leaves and rhizomes of *T.*
227 *palustris* and *T. latifolia* plants, grown in the pilot wetland system, were analyzed by light and
228 transmission electron microscope (TEM).
229 Histological observations showed that before metal exposure (T0), *T. latifolia* adult leaves
230 showed large air chambers (Fig. S2A; ac), located between two bilayered mesophylls located on
231 the upper (adaxial) and lower (abaxial) leaf sides (Fig. S2A; see Supplementary material). In the
232 mesophyll facing the monolayered epidermis, a multilayered palisade parenchyma (Fig. S2A, B,
233 C, D; bracket) was observed with small cells rich in chloroplasts separated by small intracellular

spaces. In the inner part of mesophyll, facing the large air chambers, parenchyma was formed by two layers of large isodiametric cells without chloroplasts and with large vacuoles. These cells were close to each other and extended to form the inner scaffold connecting the adaxial and abaxial leave sides (Fig. S2A, B). Vascular bundles were distributed in all the parenchymatic tissues (Fig. S2B, D, arrows).

A similar morphology of leaves was observed in T2 plants both in the control and treated samples, suggesting that exposure to metals did not lead to morphological changes in *T. latifolia* leaves (Fig. S2, compare A-D; E, F; H, I). TEM observations of chloroplasts showed thylakoids and starch granules in the control and treated plants, and did not show any alterations in organelle morphology after metal exposure (Fig. S2 G, J).

Thelypteris palustris leaves showed a different morphology in the control with respect to the treated plants (Fig. 1).

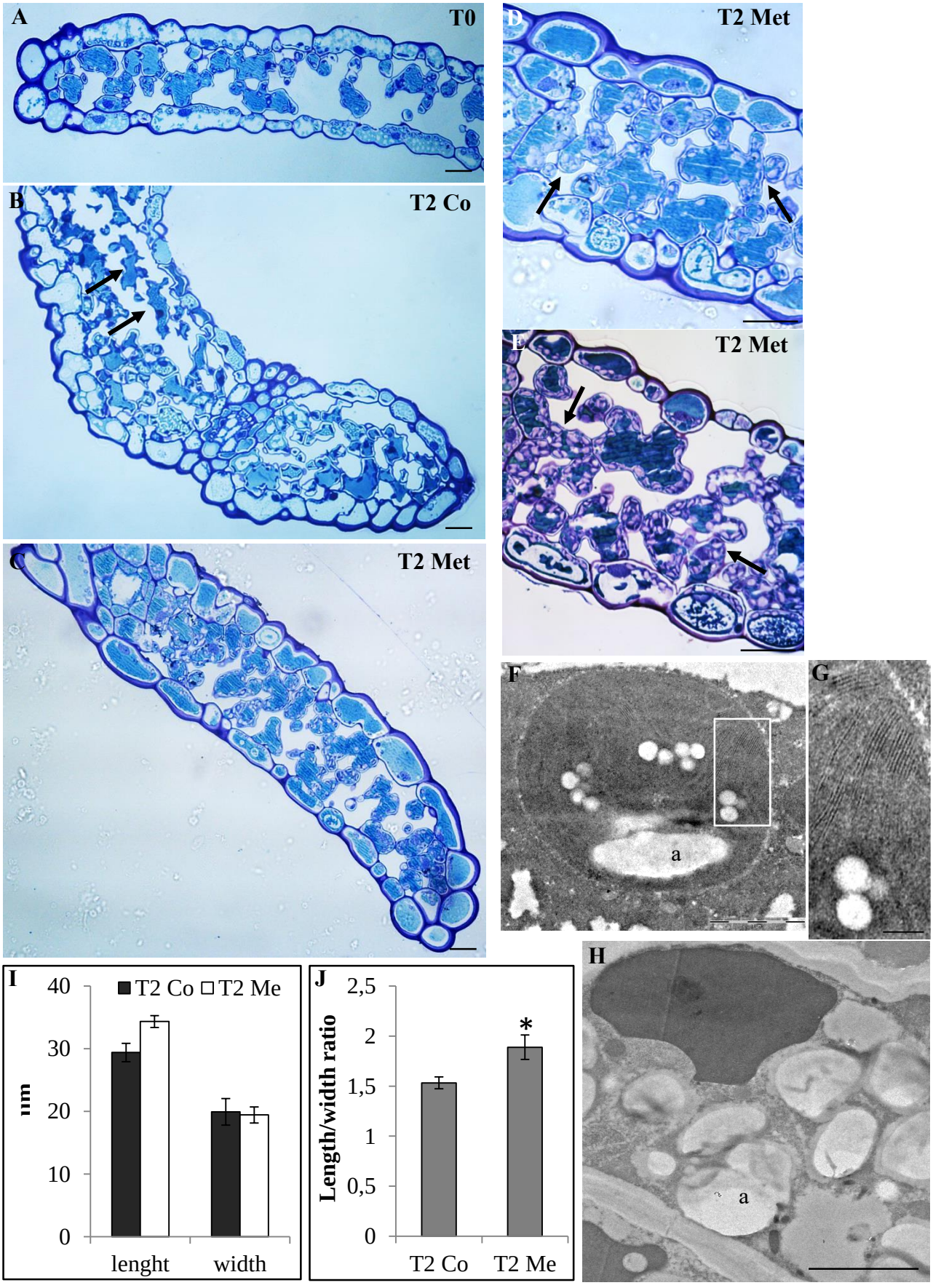
A
T0
B
T2 Co
C
T2 Met
D
T2 Met
E
T2 Met
F
a
G
H
a
I
T2 Co
T2 Me
40
30
20
10
0
lenght
width
J
2,5
2
1,5
1
0,5
0
Length/width ratio
*
T2 Co
T2 Me

Fig. 1

Fig. 1. (A) Histological observations of *T. palustris* leaves at T0. **(B)** Hystological observations of T2-Co *T. palustris* leaves; differentiated parenchymatic cells with a lobed profile are indicated by arrows. **(C-E)** Histological observations of T2-Met *T. palustris* leaves; amyloplasts accumulating in parenchyma and epidermal cells are indicated by arrows. Older leaves were showed in (E). **(F-H)** TEM observations showed that whereas in T2 Co cells chloroplasts showed well developed grana thylakoids (F, G), in T2-Met plants, a greater number of large starch grains was observed in mesophyll cells (H). Amyloplasts are indicated by: a. **(I-J)** Graphs reporting variations in parenchymatic cell shape occurring after metal exposure. Bars: (A-E) = 10 µm; (F, H) = 1 µm; (G) = 200 nm.

In fact, in T0, the leaf was thin and the mesophyll was formed by lacunose/spongy parenchyma with large intercellular spaces delimited by isodiametric or slight-lobated cells (Fig. 1A). In T2 control samples (T2-Co), parenchymatic cells were more differentiated with an extremely lobed/indented profile (Fig. 1B; arrows), while in T2 samples after metal treatment (T2-Met), the cells showed a linear profile and maintained a similar shape to that observed in T0 (Fig. 1C). In addition, there was a reduction in intracellular spaces with respect to T0.

To better define the cell shape variation, the cell size was calculated by measuring both their major (length) and minor axis (width), in sections obtained from three different leaf samples. Metal exposure led to an increase in cell length ($p=0.053$) and thus a significant difference in length/width ratio ($p<0.01$), confirming that there is a variation in parenchymatic cell shape after metal exposure (Fig. 1I, J). The similarity of T2-Met parenchyma cells with those of T0 leaves suggested that the metal treatment affected cell enlargement/differentiation, during the leaf development.

Microscopic analyses showed that in parenchymatic and epidermal cells, an accumulation of starch granules occurred in the chloroplast (Fig. 1D). In older leaves, this starch accumulation was enhanced and a great number of amyloplasts accumulated in the cells (Fig. 1E; arrows). The

conversion of chloroplasts into amyloplasts was confirmed by TEM observation: in T2 control cells (Fig. 1F, G) chloroplasts showed well developed grana thylakoids, a few starch grains and some plastoglobules as observed in T0 (data not shown). In treated plants, the mesophyll cells showed a greater number of large starch grains, while the thylakoid membrane systems disappeared (Fig. 1H), suggesting a transition from chloroplasts to amyloplasts.

3.2 Rhizome morphological alterations in response to metal treatment were similar in *T. latifolia* and *T. palustris*

Typha latifolia T0 rhizome was surrounded by a uniseriate epidermis (Fig. S3A; ep), and by a multiseriate hypodermis with large irregular cells (Fig. S3A; hp; see Supplementary material). The most significant characteristic was the presence of an outer cortical region and a central core showing different parenchymatic tissues (Fig. S3). The cortex was occupied by an aerial parenchyma (AP) formed by highly vacuolated large cells with different geometries, a thin cell wall and a few plastids (Fig. S3B). These cells were separated by large irregular intercellular spaces forming air ducts (see asterisks). Small vascular bundles (vb) were widespread in all the cortical areas (Fig. S3B).

In the inner rhizome, a storage parenchyma (SP; Fig. S3C) was found formed by isodiametric cells with numerous amyloplasts (Fig. S3C; see arrow) and small intercellular spaces. A ring of large vascular bundles defined the surface demarcating these two parenchyma (Fig. S3C; see bracket). In T2-Co and T2–Met plants, the morphology of AP and SP did not change (Fig. S3; compare F-I and E-H) and the cell dimension of SP was the same in both samples ($p>0.05$). However, after metal treatment, in the SP there was a significant decrease in the number of amyloplasts in the treated samples compared to the control (Fig. S3F, I; see arrows). Staining with Sudan Black revealed starch grains. Although no significant differences were observed in starch grain content in the T0 and T2-Co samples (Fig. 2A, B; the amount of amyloplasts was calculated by counting them in sections obtained from rhizomes of three different plants; $p>0.05$), after metal

treatment, a significant decrease in amyloplasts was evident (Fig. 2C), suggesting the influence of metals in carbohydrate accumulation.

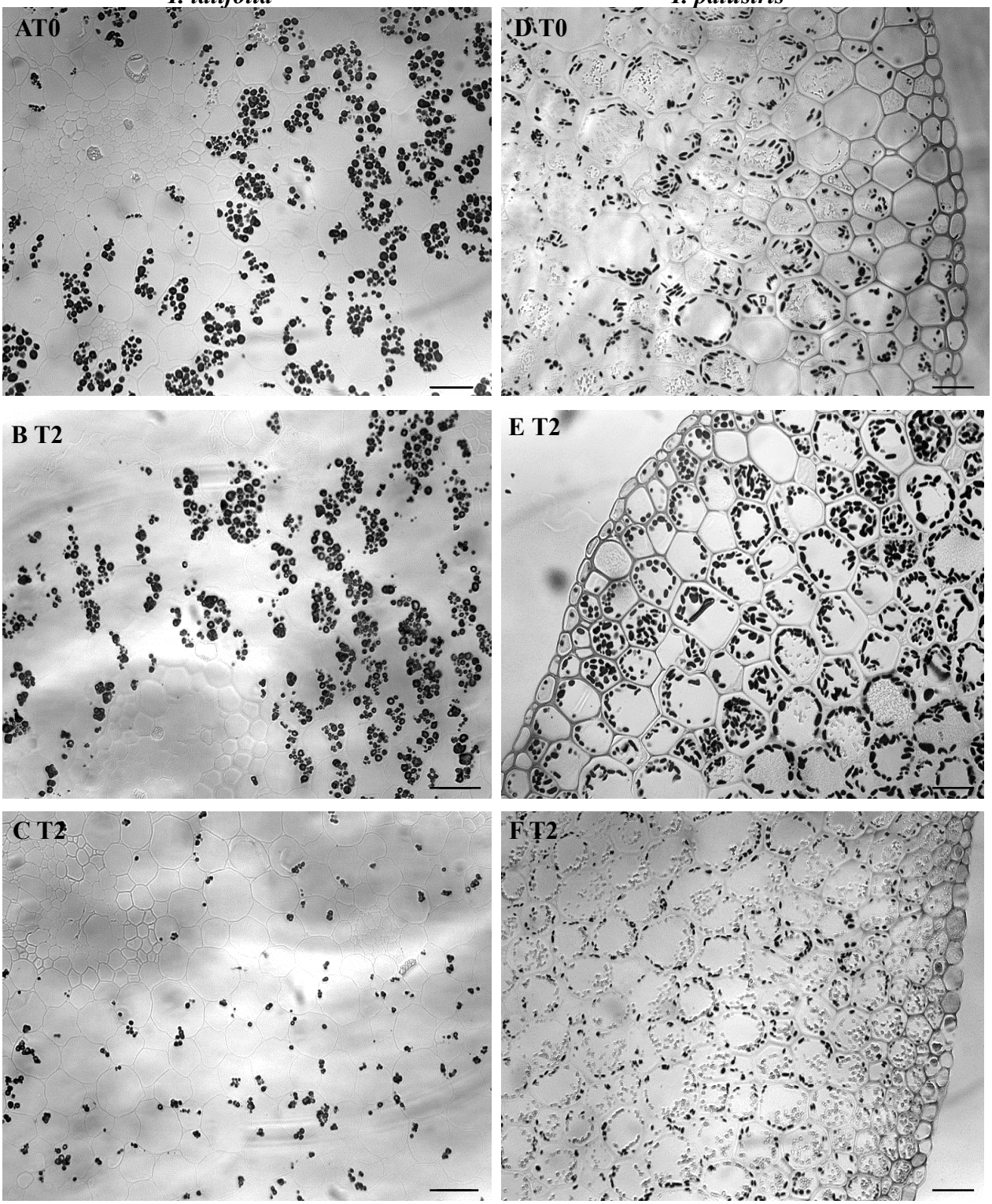

Fig. 2

Fig. 2 Sudan Black staining of *T. latifolia* rhizomes **(A-C)** No differences were observed in starch grain content in rhizomes of T0 and T2-Co samples (A, B). After metals treatment a significant decrease in the number of amyloplasts was evident (C). Sudan Black staining of *Thelypteris palustris* rhizomes **(D-F)** parenchymatic T2-Co cells showed an increase of amyloplasts with respect to T0 (D, E). A decrease of starch grains was observed after metal treatment with respect to control (F). Bar = 20µm.

In T2 samples, AP and SP were separated by an endoderm-like layer (McManus et al, 2002), with cells showing thickening in the radial and inner tangential cell wall (Fig. S3E, H; arrow). Along the endoderm-like layer, in the SP, the ring of large vascular bundles was always present (Fig. S3E, H; bracket). After metal treatment (T2-Met), the endoderm cells showed a reduction in cell wall thickening compared to the T2-Co samples (Fig. S3E, H). T2-Met and T2-Co rhizomes were observed by TEM (Fig. 3 A-F), thus confirming the differences in cell wall structure. In the AP of both treated and control samples, the cell wall was very thin and convolved. Cells were entirely occupied by large vacuoles and rare starch grains were observed (Fig. 3A, D).

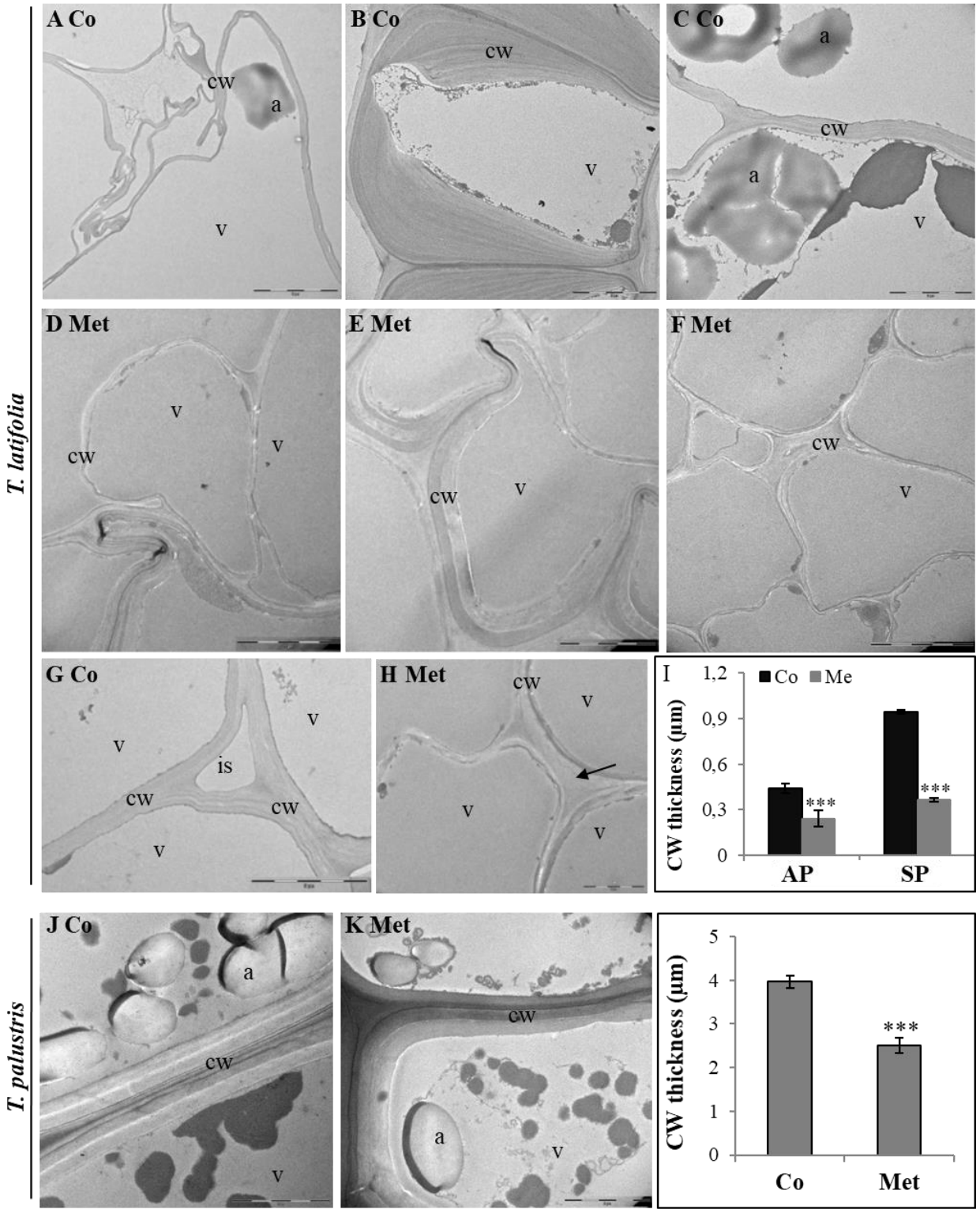

Fig. 3

Fig. 3 TEM observation of *T. latifolia* T2-Co and T2-Met rhizomes. **(A-C)** In T2-Co, the AP cell wall (cw) is thin and convolved. Cells are mostly occupied by large vacuoles (v) and rare starch grains (a) are observed (A). The T2-Co endoderm cells showed radial and inner tangential thick

cell wall, showing lamellate structure (B; cw). In the SP, cell walls were thicker with respect to AP (C; cw). **(D-F)** In T2-Met, SP cell walls were thinner (E) and a higher number of starch grains was observed in control with respect to treated cells (C, F). **(G-I)** The middle lamella in cell corners was partially reabsorbed in control samples creating intercellular spaces (G; is), while in treated samples the middle lamella persisted and cellular spaces did not form (H; arrow). The analysis of cell walls in AP and SP, showed that cell wall thickness significantly decreased ($p<0.01$) after metal treatment (I). TEM observation of *T. palustris* T2-Co and T2-Met rhizomes**. (J, K)** Parenchymatic cell vacuoles (v) were filled with dense material in both samples while and amyloplasts (a) were present in higher amount in T2-Co with respect to T2-Met. **(L)** A decrease of cell wall (cw) thickness was observed in T2-Met with respect to T2-Co. Bar = 5 µm

The endoderm cells appeared very different in T2-Met and T2-Co rhizomes (Fig. 3B, E). In fact, the cell walls of the control samples showed a very think radial and inner tangential cell wall, showing a lamellate structure (Fig. 3B; cw). On the other hand, after metal treatment, cell walls were thinner (Fig. 3E), suggesting a different cell wall deposition and remodeling. In the SP, cell walls were thicker with respect to AP (Fig. 3C, F, I) and there were more starch grains in the control than in the treated cells (Fig. 3C, F), confirming the observations made with the light microscopy. The middle lamella in the cell corners was partially reabsorbed in the control samples creating intercellular spaces (Fig. 3G), while in the treated samples the middle lamella remained and cellular spaces did not form (Fig. 3H; arrow). Alterations in cell wall structure were also confirmed by analysis of the cell wall thickness (Fig. 3I). Both in AP and SP, the cell wall thickness significantly decreased by 45% and 60%, respectively, ($p<0.01$) after metal treatment, suggesting an influence on the cell wall deposition and modification/remodelling.

In the rhizomes of *T. palustris*, both optical observations showed the presence of large vascular bundles (Fig. S4B, D, F; vb; see Supplementary material). In T0 and T2-Co samples, cortical and pith parenchymatic cells appeared isodiametric with small intercellular spaces and

were rich in starch grains (Fig. S4A-D). In the large vacuoles, dense material was often observed (Fig. S4A, C; asterisks). Rhizomes in T2-Met plants appeared morphologically similar to Co (Fig. S4E, F) and the analysis of the cell dimension did not show significant differences in cell size ($p>0.05$). However, Sudan black staining showed an increase in amyloplasts in parenchymatic T2-Co cells with respect to T0 (Fig. 2D, E) and a decrease in starch grains after metal treatment (Fig. 2F), as already observed in *T. latifolia*. This thus suggests that also in *T. palustris,* metals led to a modification in carbohydrate accumulation.

TEM observations showed that parenchymatic cell vacuoles were filled by dense material, and amyloplasts were present in higher amounts in T2-Co with respect to the treated sample (Fig. 3J-L). Similarly, *T. palustris* cell walls were different in the parenchymatic cells of T2-Co and T2-Met plants. In fact, metal treatment decreased the cell wall thickness by 40 %, suggesting the influence of metals on cell wall remodeling (Fig. 3L). In roots, which have been reported to be involved in metal accumulation (Almeida et al., 2017; Klink 2017; Klink et al., 2013), no difference in morphology was observed in treated plants with respect to controls, both in *T. latifolia* and *T. palustris* (data not shown).

3.3 Metals induce remodeling of cell walls in rhizomes of *T. palustris* but not in *T. latifolia* plants

To better define cell wall changes following metal treatment, two antibodies against high esterified (JIM7; high esterified pectins: HEPs) and low esterified pectins (LM19; low esterified pectins: LEPs) were used in indirect immunofluorescence assays. Control experiments performed without primary antibodies showed only a very low fluorescence signal in the rhizome tissues of both plants (Fig. S5; see Supplementary material).

In T2-Co *T. latifolia* plants, LM19/JIM7 antibodies showed that AP cells contained both low and high esterified pectins in the walls of rhizome cells (Fig. 4 and Fig. 5A, C, E, G respectively).

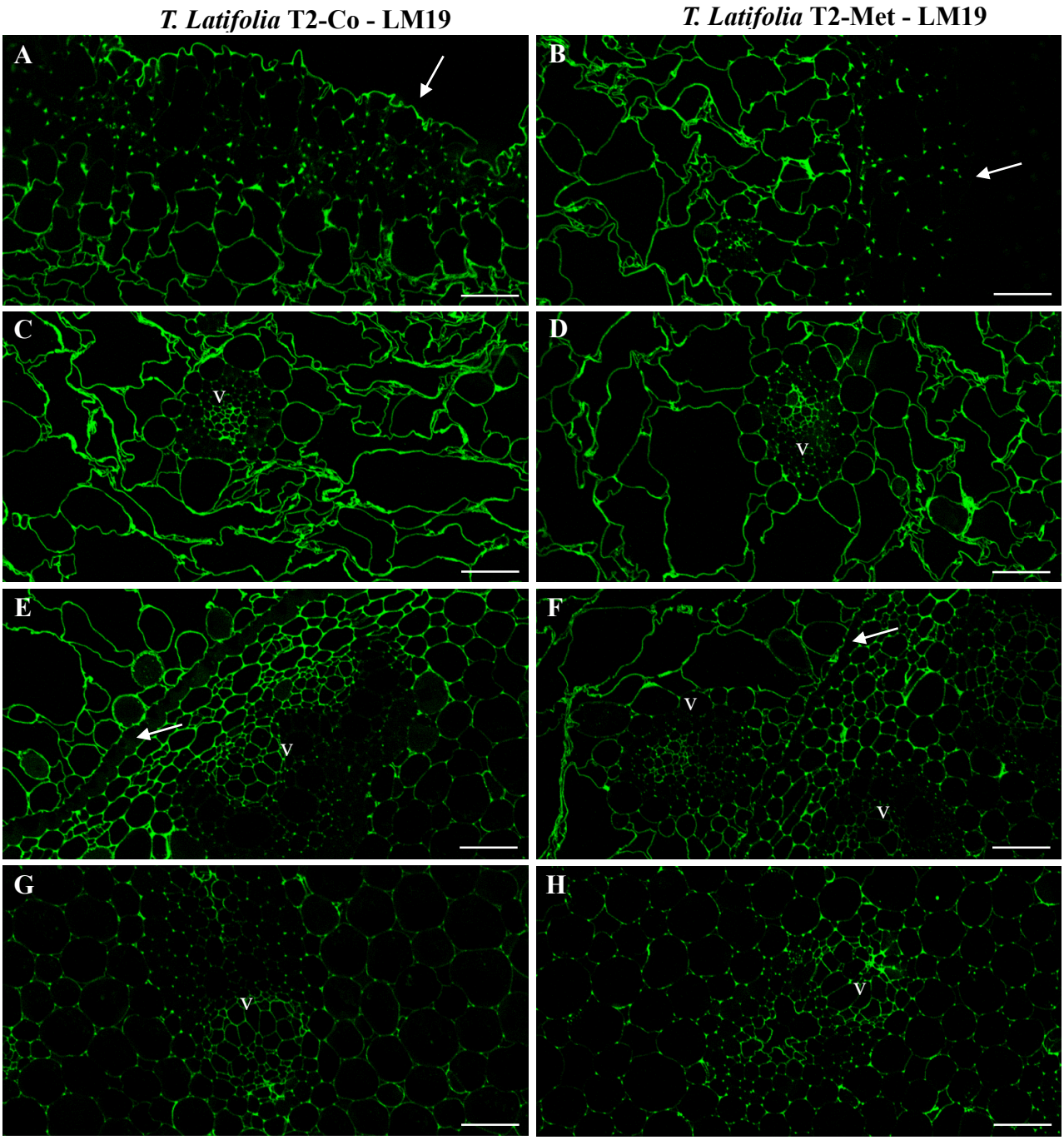

Fig. 4

Fig. 4 Distribution of LEPs in T2-Co and T2-Met of *T. latifolia* rhizomes. **(A, C, E, G)** LEPs distribution appeared continuous (C). In the SP, LEPs appeared localized mostly at the cell wall corners (G). The same distribution at the corner wall was observed in the hypodermis (A). In the epidermis, LEPs decorated the outer cell wall (A; arrow). in the endoderm LEPs were nor detected (E; arrow). In vascular bundles (vb) pectins were distributed in the vascular and parenchymatic tissues and not in sclerenchyma. **(B, D, F, H)** In T2-Met, AP, SP and endoderm did not show relevant differences in LEPs with respect to control. The only modification of cell

wall was observed in the epidermis where LEPs disappeared completely by the outer cell wall (B; arrows). Bar = 20 µm

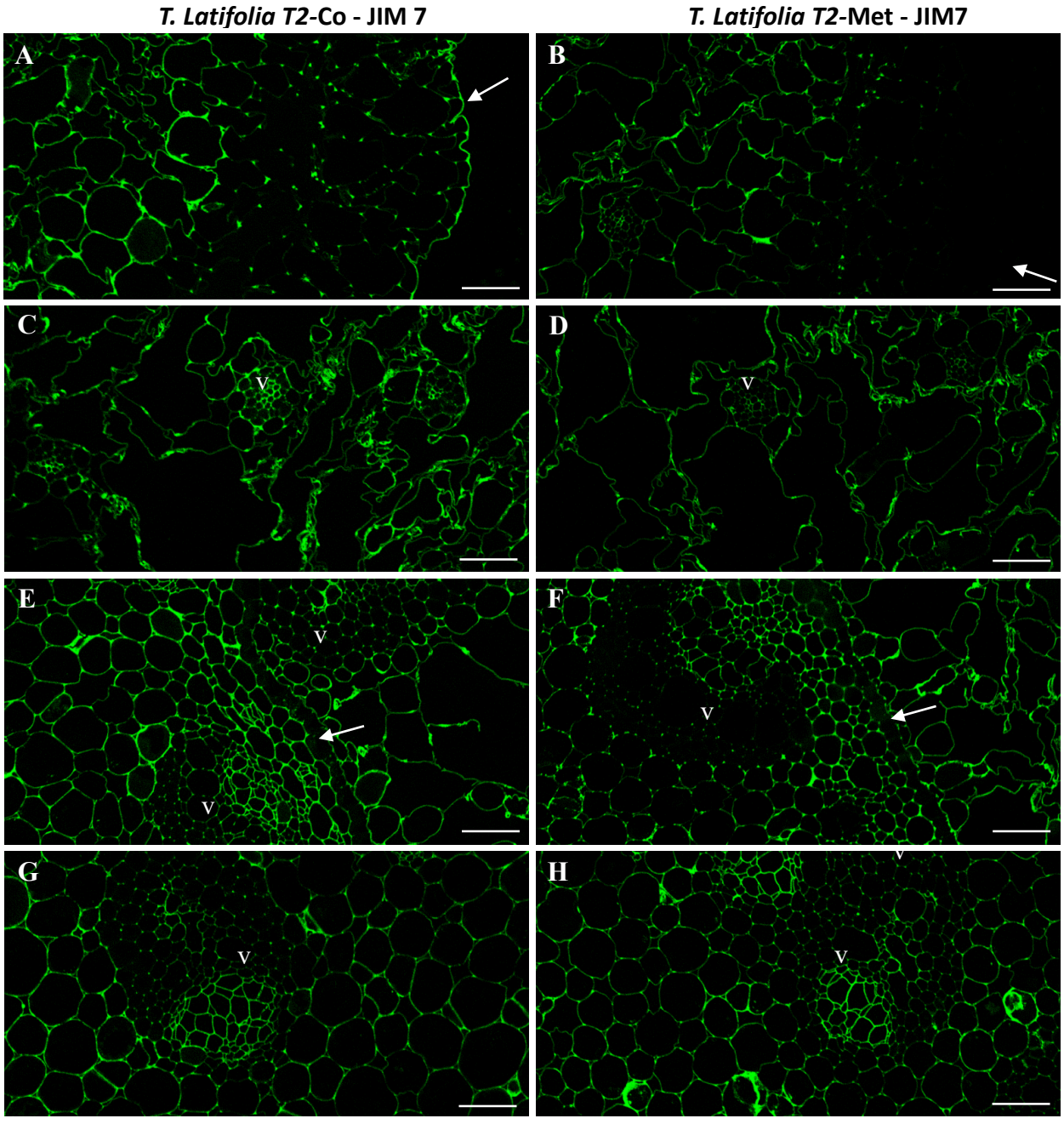

Fig. 5

Fig 5 Distribution of HEPs in T2-Co and T2-Met *T. latifolia* rhizomes. **(A, C, E, G)** HEPs distribution appeared discontinuous as they concentrated in small cell wall tracts (C). In the SP, HEPs were uniformly distributed in the cell wall (G). In the hypodermis HEPs were present at the corner of cell wall (A), while in the epidermis HEPs stained outer cell wall (A; arrow). In the

endoderm no HEPs were detected (E; arrow). **(B, D, F, H)** Immunofluorescence by using JIM7 antibody in T2-Met showed that HEPs distribution was not altered in AP and SP with respect to T2-Co. On the contrary, HEPs disappeared from the epidermis and hypodermis cell wall (B; arrow). Bar = 20 µm.

In particular, the distribution of HEPs was more discontinuous than the LEPs, as the HEPs were concentrated in small cell wall tracts (compare Figs. 4C and 5C). On the other hand, in the SP, HEPs were uniformly distributed in the cell wall, while LEPs were mainly located in the cell wall corners (Figs. 4G and 5G). The same distribution in the corner wall was observed in the hypodermis for both low and high esterified pectins (Figs. 4A and 5A). In the epidermis, both pectins were shown in outer cell wall (Figs. 9A and 10A; arrows), while in the endoderm, no pectins were recorded (Figs. 4E and 5E). In vascular bundles (Fig. 4; vb) pectins were distributed in the vascular and parenchymatic tissues and not in the sclerenchyma.

After metal treatment (T2-Met), AP, SP and endoderm did not show significant differences in LEP and HEP distribution (Figs. 4D, F, H; Fig. 5D, F, H). Interestingly, the most significant modification in the cell wall was observed in the epidermis where both pectins disappeared completely from the outer cell wall (Figs. 4A, B; Fig. 5A, B), while only HEPs disappeared from the hypodermis cell walls.

Thelypteris palustris revealed a more extensive modification of LEPs and HEPs in the rhizomes. In T2-Co samples, LEPs were distributed in the cell wall of parenchyma and in the parenchymatic cells inside the vascular bundles (Fig. 6A, C, E).

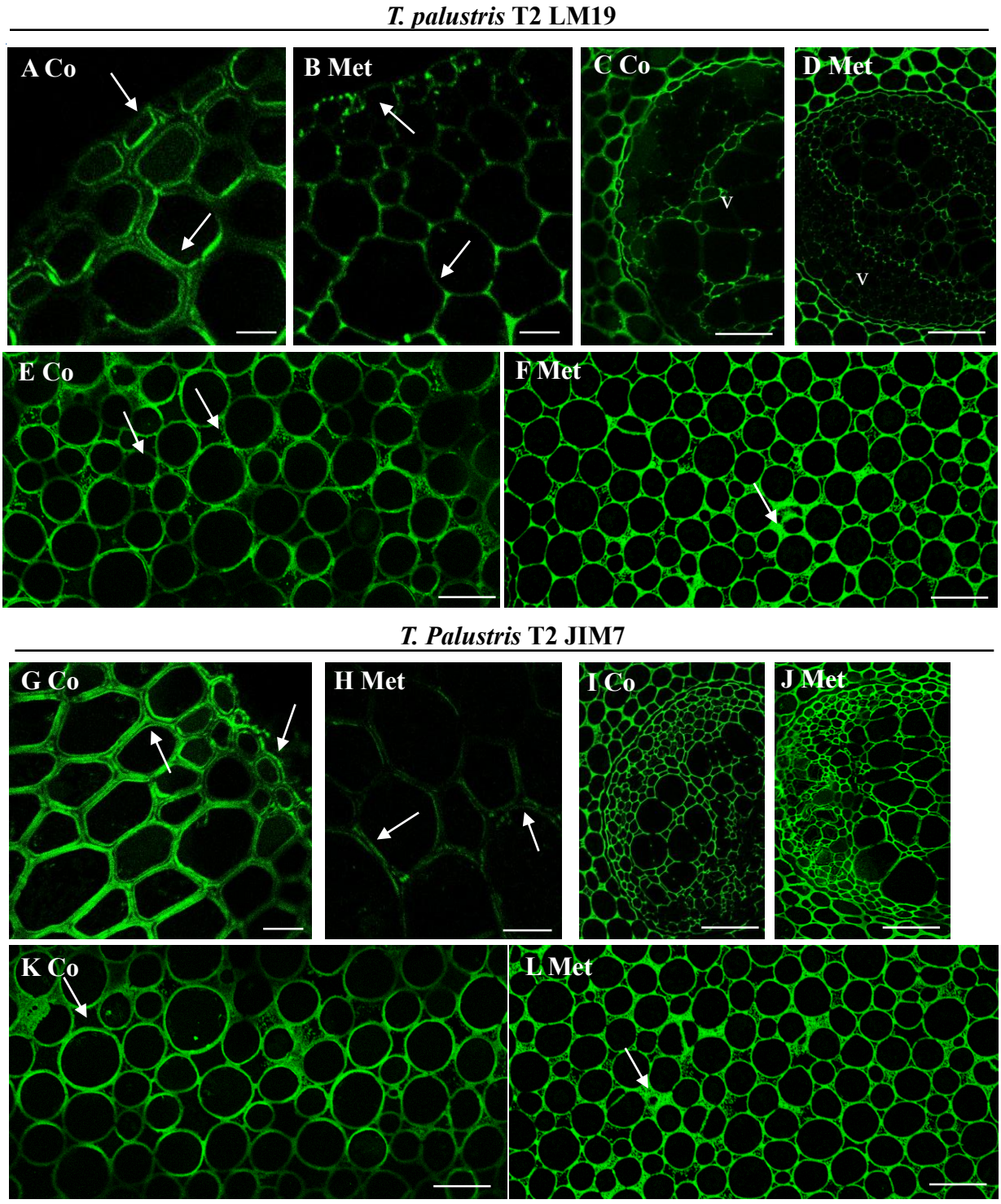

Fig. 6

Fig. 6 Distribution of LEPs and HEPs in T2-Co and T2-Met of *T palustris* rhizomes. **(A, C, E)** LEPs were distributed in the cell wall of parenchyma and in the parenchymatic cells inside the vascular bundles. In the epidermis and cortex LEPs localized in the inner layer of the primary cell wall and in the middle lamella (A; arrow). LEPs appeared uniformly distributed in the cell wall of pith cells and in parenchymatic cells surrounding xylem (C; arrows; vb: vascular bundle).

The middle lamella was reabsorbed in the corners among cells (E; arrows). **(B, D, F)** In T2-Met rhizomes LM19 stained only the middle lamella (B; arrows). In pith cells, LEPs localized in the corner among the cells, with a reduction of intercellular spaces (F; arrows). In vascular bundles the staining was similar to Co (D). **(G, I, H**) In T2-Co cortical cells HEPs were distributed in the inner layer of primary cell wall and in the middle lamella (A; arrows). In pith cells HEPs were uniformly distributed in the cell wall, excluding the corners, filled by intracellular spaces (K). In vascular bundles all the cells showed a uniform HEPs distribution (I; vb). **(H, J, L)** In T2-Met rhizomes HEPs disappeared from the middle lamella, so only the inner layer of primary cell wall was stained by JIM7 antibody (H; arrows). In the pith, HEPs persisted in the corners among cells, so reducing the extent of intercellular spaces (L; arrow), while they maintain a uniform distribution inside the vascular bundle (J; vb). Bars: (C-F, I-L) = 20 µm; (A, B; C, H) = 10 µm

In the epidermis and cortex, LEPs were located in the inner layer of the primary cell wall and in the middle lamella (Fig. 6A; arrows). The primary cell walls close to the middle lamella did not show LM19 staining (Fig. 6A). The low esterified pectins were uniformly distributed in the cell wall of pith cells and in the parenchymatic cells surrounding xylem (Fig. 6C, E). In the corners of cells, the middle lamella was reabsorbed creating intercellular spaces (Fig. 6E; arrows). After metal treatment, in the epidermis and cortex, LM19 stained only the middle lamella (Fig. 6B; arrows), while in the pith cells, LEPs were found in higher amounts in the corner of the cells, causing a reduction in intercellular spaces (Fig. 6F; arrow). No modifications were observed in the vascular systems (Fig. 6D).

HEP location also changed after metal treatment (Fig. 6G-L). In T2-Co samples, cortical cells showed a distribution of HEPs in the inner layer of the primary cell wall and in the middle lamella (Fig. 6G; arrows). Metal treatment led to the disappearance of HEPs from the middle lamella, thus only the inner layer of primary cell wall was stained by the JIM7 antibody (Fig. 6H; arrows). In T2-Co pith cells, the HEPs were uniform in the cell wall, excluding the corners of cells filled by

557 intercellular spaces (Fig. 6K). In the vascular bundles all the cells showed a uniform HEP
558 distribution (Fig. 6I). As observed for LEPs, in T2-Met cells, HEPs remained in the corners of
559 cells, thus reducing the extent of intercellular spaces (Fig. 6L; arrow), while they maintained the
560 same distribution inside the vascular bundle (Fig. 6J).
561
562 **3.4 Protein analysis by 1D- and 2D-gel electrophoresis and protein identification.**
563 To investigate the molecular basis of cell walls and starch modification observed after
564 metal treatment, we compared the protein profiles of leaves and rhizomes of the control and treated
565 *T. latifolia* and *T. palustris* (T2-Me compared to T2-Co) by 1D-gel electrophoresis.
566 In the leaves of both plants, 1-D electrophoresis did not reveal qualitative and quantitative
567 differences in the protein profile (compare Fig. 7A and B).

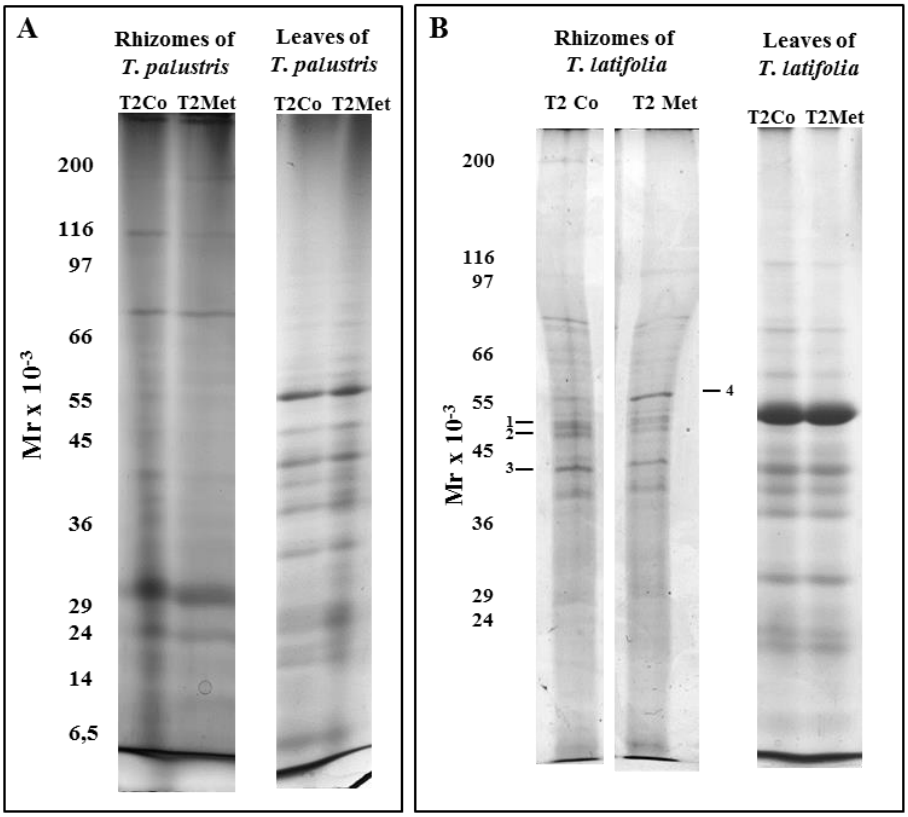

Band	Protein description	Accession number	Database	Mascot search results			Organism
				Score	Sequence coverage (%)	N. of matched peptides	
1	Tubulin beta-2 chain	TBB2_SOYBN	SwissProt	174	47	24/65	*Glycine max*
2	Tubulin alpha chain	TBA_DAUCA	SwissProt	203	46	20/40	*Daucus carota*
3	Actin-104 (Fragment)	ACT7_TOBAC	SwissProt	156	56	18/65	*Nicotiana tabacum*
4	Cullin-3B Lysine-specific demethylase JMJ25 Pentatricopeptide repeat-containing protein At2g36730	CUL3B_ARATH JMJ25_ARATH PP188_ARATH	SwissProt	98 61 58	31 26 34	28/114 23/114 15/114	*Arabidopsis thaliana*

Fig. 7 One-dimensional gel electrophoresis and mass spectrometry. **(A)** Electrophoretic profile of *T. palustris* T2-Co and T2-Met rhizome and leaves extracts. **(B)** Electrophoretic profile of *T. latifolia* T2-Co and T2-Met rhizome and leaves extracts. 20 µg of protein was loaded in each lane. **(C)** Proteins differentially expressed in T2-Co and T2-Met T. latifolia rhizomes.

Similarly, control and treated rhizomes of *T. palustris* did not show differences in the 1-D gel electrophoresis protein profile (Fig. 7A). On the other hand, in *T. latifolia* rhizomes exposed to metals, 1-D electrophoresis showed a decrease in proteins with a molecular mass of between 40

577 and 55 kDa (Fig. 7B; compare T2 Co and T2 Me; bands 1, 2, 3) and an increase in a 56 kDa protein
578 (Fig. 7B; compare T2- Co and T2-Met; bands 4) in comparison to the controls. These polypeptides
579 were excised from 1-D gels and subjected to MALDI TOF/TOF MS analysis (Fig 7C).
580 Interestingly, mass spectrometry identified proteins belonging to the cytoskeletal system:
581 β- and α-tubulin were identified in bands 1 and 2 respectively, and actin was identified in band 3,
582 suggesting that metals induced a decrease in cytoskeletal proteins in treated plants (Fig 7C). In the
583 increased band 4, three different proteins were detected: cullin 3B; lysine-specific demethylase
584 JMJ125 and pentatricopeptide repeat-containing protein (Fig 7C). Although it is not possible to
585 differentiate whether all or only one protein determined the increase in band 4 intensity, the
586 molecular weight of pentatricopeptide repeat-containing protein was consistent with the band
587 position in the gel (about 56 kDa). Cullin 3B and Lysine-specific demethylase JMJ125 proteins
588 presented a lower molecular weight with respect to findings reported in the data bank.
589
590 **5. DISCUSSION**
591 Animal production is a source of heavy metal contamination in the environment through the reuse
592 of treated wastewaters for agricultural purposes. These waters contain substantial concentrations
593 of metals, which are generally above the legal limits for irrigation. Innovative approaches are thus
594 needed in order to make intensive livestock more sustainable.
595 Mechanisms based on tolerance and metal uptake/accumulation are species specific (Hasan
596 et al., 2017; Kumar and Tivedi, 2016; Oves et al., 2016; Singh et al., 2016; Viehweger, 2014;
597 Yadav, 2010). Through the integrated use of cell biological techniques, here we demonstrate that
598 *T. palustris* and *T. latifolia,* deal in different ways with heavy metals with specific molecular
599 responses.
600
601 **5.1 Metal exposure induces alteration of *T. palustris* leaf ultrastructure and affects**
602 **carbohydrate metabolism of both *T. palustris* and *T. latifolia*.**

603 Neither the leaf nor rhizome biomass of *T. palustris and T. latifolia*, were affected by the
604 presence of metals (see accompayning paper, Hejna et al., 2019). Concerning *T. latifolia*, this result
605 was expected since the Zn^{2+} and Cu^{2+} concentrations used in our experiment were below the
606 tolerance thresholds identified by Manios et al. (2003).

607 In agreement with the lack of macroscopic alterations, no microscopic modifications
608 occurred in the leaves of *T. latifolia* after 45 days of metal treatment. However, although
609 symptomless in macroscopic morphology, *T. palustris* showed changes in mesophyll cell
610 morphology. A similar cell shape to young T0 mesophyll leaf cells, was observed in *T. palustris*
611 leaves after metal exposure (T2-Met), suggesting a delay in leaf cell differentiation. In bean
612 (*Phaseolus vulgaris*), a low dose of heavy metals (Cd, Pb, Ni, Ti) was shown to induce a
613 rejuvenating effect on leaves (Nyitrai et al, 2004). It was hypothesized that this process could be
614 due to an increasing cytokinin concentration induced by low-dose stressors which generate a non-
615 specific alarm reaction (Nyitrai et al, 2004). In *T. palustris*, altered leaf cell shape was
616 accompanied by an accumulation of starch grains which suggested a transformation of chloroplasts
617 into amyloplasts.

618 All these data are supported by chemical analyses showing an increase in starch in the
619 aerial organs (accompayning paper, Hejna et al., 2019). The accumulation of starch in the leaves
620 could be due to changes in carbohydrate metabolism. In fact, in several plants, metal exposure
621 causes a variation in photosynthetic process accompanied by significant alterations in plant
622 biomass and leaf morphology/ultrastructure (Arif et al, 2016; Rufner and Barker, 1984;
623 Stoláriková-Vaculíková et al., 2015; Todeschini et al, 2011). One of the mechanisms of metal
624 tolerance has been shown to be the accumulation of metals in the ageing leaves (Małachowska-
625 Jutsz and Gnida 2015). The higher accumulation of amyloplasts in older with respect to younger
626 leaves, also suggested that in *T. palustris*, such stress avoidance may occur. However, *T. palustris*
627 did not show a decrease in biomass suggesting that, although chloroplasts were transformed into
628 amyloplasts, the plants grew normally.

In most plants, high copper exposure disorganizes the chloroplast ultrastructure without starch accumulation (Maksymiec et al., 1996), while in screwbean mesquite, excess copper affects chloroplast development leading to starch accumulation in cotyledons (Zappala et al, 2014). However, this starch accumulation was induced by a much higher copper concentration (400 mg/L) than the one used in our model (8.63 mg/L). In addition, in detached bean leaves, a low-dose of Pb and Ni increased the starch content without significantly affecting photosynthetic activity (Nyitrai et al., 2004). In *T. palustris*, starch accumulation did not affect plant growth and did not induce discoloration or chlorosis in leaves.

An alternative hypothesis for the presence of amyloplasts in leaves could be due to a modification of carbohydrate translocation away from leaves. This hypothesis was supported by the decrease in starch granules in the rhizomes in treated plants with respect to the control, as also confirmed by chemical analyses (see accompayning paper, Hejna et al., 2019). In screwbean mesquite, the increase in copper was accompanied by a decrease in potassium concentration (Zappala et al, 2014). Interestingly, the alteration of Na and K homeostasis, disturbed phloem loading and translocation, leading to an accumulation of starch in Arabidopsis leaves (Tian et al, 2010). Further experiments would be necessary to better clarify this point in *T. palustris*.

In *T. latifolia*, no differences were observed in the leaves of T2-Met with respect to T2-Co plants. However, the starch accumulation in rhizome decreased, as also confirmed by chemical analyses (see accompayning paper, Hejna et al., 2019). Unlike *T. palustris*, the starch reduction could be due to different mechanisms not involving phloem translocation and loading. In *Cucurbita pepo*, a higher Zn^{2+} concentration was correlated with an increase in soluble sugars and a decrease in starch in roots and shoots (Ialelou et al, 2013). The increase in soluble sugars in stressed plants is considered to be important for preserving biological molecules and membranes (Gibson, 2005). In addition, although direct evidence of the effect of high Zn^{2+} concentration on the starch synthesis enzymes was lacking, zinc deficiency has been found to reduce the starch

synthase activity (Ialelou et al, 2013). Further analyses could clarify whether the same inhibitory effect on starch synthesis enzymes also occur at high metal concentrations.

In *T. latifolia* and *T. palustris*, rhizome carbohydrate metabolism alterations therefore appeared to be caused by different mechanisms.

Although the carbohydrate metabolism was different in the control and metal treated cells, proteomic analysis did not show alterations in the polypeptides involved in carbohydrate metabolism or translocation. In addition, *T. palustris*, which changed above all in leaf morphology after metal exposure, did not show differences in the polypeptide profile in 1D-gel electrophoresis.

5.2 Cell wall remodeling in rhizomes was related to metal exposure of *T. latifolia* and *T. palustris*

In plants that accumulate metals, there are various strategies to prevent toxicity. One strategy is sequestration into extra-cytoplasmic compartments such as the cell wall. Cell wall polysaccharides play a major role in binding and accumulating metals in order to remove them from protoplasts (Jiang and Wang 2008; Le Gall et al, 2015). In different plant phytoremediation models, metal exposure induces a thickening of the cell wall and pectin remodeling by modulating the degree of melthylesterification, thus affecting the ability of the cell wall to bind metals (Dronnet et al, 1996; Eticha et al, 2005; Krzeslowska, 2011; Le Gall et al, 2015). Previous studies have shown that Cu^{2+} and Zn^{2+} have a high affinity for low esterified pectins and replace Ca^{2+} ions in the pectin matrices (Dronnet et al, 1996). Metal exposure has been found to enhance cellulose, hemicellulose and pectin content in the cell walls and induce the up-regulation of CesA and XTH genes (Gao et al. 2013; Liu et al, 2014).

Unlike most plants used for phytoremediation, *T. latifolia* and *T. palustris* showed a significant reduction in cell wall thickening in rhizomes after metal exposure. This cell wall thinning could be associated with a dysfunction of cytoskeleton due, for instance, to a MT reduction as that observed in *T. latifolia* rhizomes after metal exposure. Microtubules (MTs) and

680 actin filaments (AFs) were found to be involved in secretion processes necessary for plant cell
681 wall building. Pectin, hemicellulose and cellulose synthase complex (CSC) were transported to
682 and out of PM by Golgi-derived secretory vesicles. Both AFs and MTs play an important role in
683 membrane trafficking and in the proper positioning of secretory vesicles carrying cell wall
684 components (Gutierrez et al, 2009; Kim and Brandizzi, 2013; Onelli et al, 2015). The decrease in
685 tubulin and actin revealed by electrophoretic analyses could be responsible for the thinning of the
686 cell wall in *T. latifolia* rhizome parenchymatic cells.

687 It has been reported that cytoskeleton is affected by Zn^{2+} and Cu^{2+}: MTs and AFs can be
688 targets of the metals, which leads to a disturbance of the organization and dynamics of cytoskeletal
689 structures in the cells (Eagle et al., 1983; Gaskin and Kress, 1977; Horiunova, and Yemets 2015;
690 Kulikova et al., 2009). Both MTs and AFs are sensitive to $Cu^{2+,}$ while Zn^{2+} only affects MTs:
691 approximately 60 potential binding sites of tubulin with Zn^{2+} have been described (Horiunova et
692 al., 2016).

693 Secretion is also important for the presence of pectin remodeling enzymes such as pectin
694 methylesterase. In plants, during maturation in Golgi cisternae, pectins have been shown (Li et al.,
695 2002) to be high-methylesterified and secreted in this form by secretory vesicles. In the cell wall,
696 pectin methylesterases could de-esterify pectins, allowing pectins to bind Ca^{2+} or other metals. The
697 increase in LEPs was an important mechanism for metal tolerance (Eticha et al, 2005; Le Gall et
698 al, 2015). In *T. latifolia* and *T. palustris* rhizomes, as expected the analyses of LEPs and HEPs
699 revealed by the use of LM19 and JIM7 antibodies respectively, did not show an increase in LEPs
700 concomitant with a decrease in HEPs.

701 In *T. latifolia*, the distribution of both pectins in the cell wall was similar in the control and
702 metal treated samples in the inner tissues, while pectins disappeared completely from the outer
703 epidermis cell wall. This slight effect of metal exposure on the extent of methyl esterification of
704 pectins was probably due to the lower metal concentration in the water. Furthermore, in *T. latifolia*
705 rhizomes, the reduction in cell wall thickness was also observed in the endodermis cells between

706 AP and SP. Abiotic stresses induce suberin accumulation in the root endodermal cell wall
707 (Andersen et al, 2015). The presence of suberin in the Casparian band was important to select the
708 uptake of nutrients and to exclude potential phytotoxic compounds. The increase in endodermal
709 cell wall suberification represents a physical barrier against the entry of metals into the symplastic
710 compartment. Again, *T. latifolia* showed a different reaction, since in the endodermis, cell walls
711 were thinner than the control. Presumably, suberin was still deposited in the cell wall, since the
712 endodermis was never stained by antibodies against LEPs and HEPs.

713 *T. palustris* had a different distribution of HEPs and LEPs in the walls of parenchymatic
714 cells. After metal treatment, HEPs were located in the inner part of the cell wall, while LEPs
715 remained only in the middle lamellae. In addition, both LEPs and HEPs remained in the corner of
716 the cells, which in control rhizomes were replaced by intercellular spaces. These data suggest that
717 the cell wall remodeling was different after metal exposure with respect to the control, although
718 no polypeptide modifications were revealed by 1D-gel electrophoresis. Modification of pectins
719 cannot be explained by the need to bind excess metal ions to prevent their entry in the symplast,
720 suggesting that these modifications are not part of a tolerance mechanism. Further analyses could
721 better define the processes affected by the metal exposure which induced modifications of the cell
722 wall in *T. palustris* rhizome.

723 In *T. latifolia*, proteomic analyses of polypeptides in 1D gel electrophoresis showed an
724 increase in a band (band 4) containing three different proteins: cullin 3B; lysine-specific
725 demethylase JMJ125 and pentatricopeptide repeat-containing protein. Pentatricopeptide repeat-
726 containing protein is the only polypeptide with a molecular mass that is in line with the molecular
727 weight of this band. It belongs to a superfamily of proteins involved in RNA editing, RNA
728 stabilization, RNA cleavage, translational activation and RNA splicing in nuclei, chloroplast and
729 mitochondria (Barkan and Small, 2014; Manna 2015). This protein was shown to be involved in
730 RNA modification in chloroplasts. A subclass of these proteins contains a domain with zinc-
731 binding capabilities (Boussardon at 2014; Hayes et al, 2013). In *T. latifolia*, these proteins may

perhaps have been susceptible to the Zn^{2+} concentrations used in our system. However, the modification of the content of this protein did not affect plant morphology or growth.

5.3 Conclusions

Typha. latifolia and *T. palustris* were able to grow and to significantly reduce the amount of Zn^{2+} and Cu^{2+} which are the main outputs of heavy metal from intensive livestock production. Metal concentrations which are fourteen times higher than Italian legal limits, were however too low to induce macroscopic morphological modifications in either of the plants. At these metal concentrations, which are in the range found in wastewaters generally used for field irrigation, both plants were successful in phytoremediation thanks to their capacity to accumulate metals within the rhizome and leaves. Our chemical analyses highlight that the two plants could be used in series to refine wastewater. However, although metal concentrations are below the toxicity limit already reported for *T. latifolia* (Klink, 2017), some tissue morphology alterations were observed in the rhizomes and leaves of both plants.

T. palustris and *T. latifolia* respond differently to the overall effect of the metals and show different cellular and biochemical characteristics, suggesting a different degree of tolerance. *T. palustris* was more sensitive than *T. latifolia*, since the modification in both the leaf and rhizome cells (cell shape, cell wall thickness and pectin distribution) and carbohydrate metabolism indicate that the marsh fern was affected the most by the presence of the two metals.

The early uptake of the metals in *T. palustris* revealed by chemical analyses (see the accompayning paper: Hejna et al., 2019) probably exposes the plants to metals for a longer period than *T. latifolia*. In fact, the accumulation of a large amount of Cu^{2+} and Zn^{2+} led to a slight toxic effect which was revealed by morphological observations without affecting plant growth.

However, it is interesting that the amount of metals in the marsh fern tissues were always higher than *T. latifolia*, also considering the increase in biomass from T0 to T2. It is possible that higher concentrations of metals or longer exposure times may cause macroscopical damage in the plants.

Thus, in *T. palustris* the metal effects appeared to be due to a slight toxicity. On the other hand, in *T. latifolia*, changes in carbohydrate metabolism appeared to be part of a tolerance mechanism, while cell wall modifications are ascribable to a metal toxic effect.

In conclusion, although further analyses are needed to clarify whether some of the morphological and biochemical alterations are due to a toxic metal effect or are part of tolerance mechanisms, the data presented suggest that *T. latifolia* showed a higher tolerance to metals than *T. palustris* and seems to be more suitable for the long-term phytodepuration of livestock wastewaters, in series with marsh ferns.

We believe that our data also provide new insights into mechanisms that have evolved in plants and that belong to different evolutionary groups, in response to the presence of heavy metals in the environment.

Funding: This study was funded by the Italian Agricultural Ministry (MIPAAF grant - LOW METAL project).

Acknowledgment

We are very grateful to Prof. Sandra Citterio for the critical reading of the paper, Dr Enrico Sala and Valerio Parravicini for the wetland system building and for taking care of *Typha latifolia* and *Theliypteris palustris* plants. We tank also Prof. Marco Caccianiga for the helpful suggestion on wetland system management.

Author Contributions

Conceptualization: Moscatelli A. Rossi L.; Data curation: Moscatelli A., Stroppa N., Onelli E.; Funding acquisition: Moscatelli A. Rossi L.; Methodology: Onelli E., Stroppa N., Gagliardi A., Bini L.; Project administration: A. Moscatelli, Supervision: A. Moscatelli; Validation: E. Onelli, L. Rossi; Writing ± original draft: E. Onelli, A, Moscatelli; Editing: M. Hejna, L. Rossi.

784

785 REFERENCES

786 1. Agenzia per la Protezione dell'Ambiente e per i Servizi Tecnici. 2006. Confronto tra
787 concentrazioni limite accettabili ex D.M.471/99 e concentrazioni soglia di contaminazione ex
788 D/Lgs 152/06.

789 2. Almeida, C.M.R., Santos, F., Ferreira, A.C., Gomes, C.R., Basto, M.C., Mucha, A.P. 2016
790 Constructed wetlands for the removal of metals from livestock wastewater - Can the presence
791 of veterinary antibiotics affect removals? Ecotoxicol Environ Saf. 137, 143-148.
792 https://doi.org/10.1016/j.ecoenv.2016.11.021.

793 3. Andersen, T.G., Barberon, M., Geldner, N. 2015. Suberization - the second life of an
794 endodermal cell. Curr. Opin. Plant Biol. 28, 9-15. https://doi.org/ 10.1016/j.pbi.2015.08.004.

795 4. Anning, A.K., Korsah, P.E., Addo-Fordjour, P. 2013. Phytoremediation of wastewater with
796 *Limnocharis flava*, *Thalia geniculata* and *Typha latifolia* in constructed wetlands. Int. J.
797 Phytorem. 15, 452-464. https://doi.org/10.1080/15226514.2012.716098.

798 5. Arif, N., Yadav, V., Singh, S., Singh, S., Ahmad, P., Mishra, R.K., Sharma, S., Tripathi, D.K.,
799 Dubey, N.K., Chauhan, D.K. 2016. Influence of high and low levels of plant-beneficial heavy
800 metal ions on plant growth and development. Front. Environ. Sci. 4, 69.
801 https://doi.org/10.3389/fenvs.2016.00069.

802 6. Barkan, A., Small, I. 2014. Pentatricopeptide repeat proteins in plants. Ann. Rev. Plant Biol.
803 65, 415-442. https://doi.org/10.1146/annurev-arplant-050213-040159.

804 7. Boussardon, C., Avon, A., Kindgren, P., Bond, C.S., Challenor, M., Lurin, C., Small, I. 2014.
805 The cytidine deaminase signature HxE (x) nCxxC of DYW1 binds zinc and is necessary for
806 RNA editing of ndhD-1. New Phytol. 203, 1090-1095. https://doi.org/10.1111/nph.12928.

807 8. Bradford, M. M. 1976. A rapid and sensitive method for the quantitation of microgram
808 quantities of protein utilizing the principle of protein-dye binding. Annal. Biochem. 72, 248-
809 254 https://doi.org/10.1016/0003-2697(76)90527-3.

9. Collin, V. C., Eymery, F., Genty, B., Rey, P., and Havaux, M. 2008. Vitamin E is essential for the tolerance of *Arabidopsis thaliana* to metal-induced oxidative stress. Plant Cell Environ. 31, 244-257. https://doi.org/10.1111/j.1365-3040.2007.01755.x.
10. Colzi, I., Arnetoli, M., Gallo, A., Doumett, S., Del Bubba, M., Pignattelli, S., Gabbrielli, R., Gonnelli, C. 2012. Copper tolerance strategies involving the root cell wall pectins in *Silene paradoxa* L. Environ Exp Bot 78, 91-98. https://doi.org/10.1016/j.envexpbot.2011.12.028.
11. Doğanlar, Z.B. 2013 Metal accumulation and physiological responses induced by copper and cadmium in *Lemna gibba*, *L. minor* and *Spirodelan polyrhiza*. Chem. Spec. Bioavail. 25, 79-88. https://doi.org/10.3184/095422913X13706128469701.
12. Dronnet, V.M., Renard, C.M.G.C., Axelos, M.A.V., Thibault, J.F. 1996. Heavy metal binding by pectins: selectivity, quantification and characterization. Carbohydr. Polym. 30, 253-263. https://doi.org/10.1016/S0921-0423(96)80283-8.
13. Dubey, S., Shri, M., Misra, P., Lakhwani, D., Bag, S. K., Asif, M. H., Trivedi, P.K., Tripathi, R.D., Chakrabarty, D. 2014. Heavy metals induce oxidative stress and genome-wide modulation in transcriptome of rice root. Funct. Integr. Genomics 14, 401-417. https://doi.org/10.1007/s10142-014-0361-8.
14. Eagle, G.R., Zombola, R.R., Himes, R.H., 1983. Tubulin–zinc interactions: binding and polymerization studies. BMC Biochem. 22, 221-228. https://doi.org/10.1021/bi00270a032.
15. Eticha, D., Stass, A., Horst, W.J. 2005 Cell-wall pectin and its degree of methylation in the maize root apex: significance for genotypic differences in aluminium resistance. Plant Cell Env. 28, 1410-1420. https://doi.org/10.1111/j.1365-3040.2005.01375.x.
16. European Parliament and the Council. Regulation (EC) no 1831/2003 of 22 September 2003 on additives for use in animal nutrition. Off J. L: 268/29.
17. Fediuc, E., Erdei, L. 2002. Physiological and biochemical aspects of cadmium toxicity and protective mechanisms induced in *Phragmites australis* and *Typha latifolia.* J. Plant Physiol. 159, 265-271. https://doi.org/10.1078/0176-1617-00639.

836 18. Gao, J., Sun, L., Yang, X., Liu, J.X. 2013 Transcriptomic analysis of cadmium stress response
837 in the heavy metal hyperaccumulator *Sedum alfredii* Hance. PLoS One, 8, e64643.
838 https://doi.org/10.1371/journal.pone.0064643.
839 19. Gaskin, F. and Kress, Y. 1977. Zinc ion induced assembly of tubulin. J. Biol. Chem. 252,
840 6918-6924.
841 20. Gibson, S. 2005. Control of plant development and gene expression by sugar signaling. J.
842 Plant Biol. 8, 93-102. https://doi.org/10.1016/j.pbi.2004.11.003.
843 21. Gutierrez, R., Lindeboom, J.J., Paredez, A.R., Emons, A.M., Ehrhardt, D.W. 2009
844 Arabidopsis cortical microtubules position cellulose synthase delivery to the plasma
845 membrane and interact with cellulose synthase trafficking compartments. Nat Cell Biol. 11,
846 797-806. https://doi.org/10.1038/ncb1886.
847 22. Hasan, K., Cheng, Y., Kanwar, M.K., Chu, X.Y., Ahammed, G.J., Qi, Z.Y. 2017. Responses
848 of plant proteins to heavy metal stress - a review. Front. Plant Sci,
849 https://doi.org/10.3389/fpls.2017.01492.
850 23. Hayes, M.L., Giang, K., Berhane, B., Mulligan, R.M. 2013. Identification of two
851 pentatricopeptide repeat genes required for RNA editing and zinc binding by C terminal
852 cytidine deaminase-like domains. J. Biol. Chem. 288, 36519-36529.
853 https://doi.org/10.1074/jbc.M113.485755.
854 24. Hellman, U., Wernstedt, C., Gonez, J. and Heldin, C. H. 1995. Improvement of an ‘‘In-Gel’’
855 digestion procedure for the micropreparation of internal protein fragments for amino acid
856 sequencing. Anal. Biochem. 224, 451-455. https://doi.org/10.1006/abio.1995.1070.
857 25. Hejna M, Moscatelli A, Stroppa N, Onelli E, Pilu S, Baldi A, Rossi L. 2019. Bioaccumulation
858 of heavy metals from wastewater through *Typha latifolia* and *Thelypteris palustris*
859 phytoremediation system. Submitted on the 19^{h} of July to Chemosphere, Manuscript Number:
860 CHEM64390

861 26. Higuchi, K., Kanai, M., Tsuchiya, M., Ishii, H., Shibuya, N., Fujita, N., Nakamura, Y., Suzui,
862 N., Fujimaki, S., Miwa, E. 2015 Common reed accumulates starch in its stem by metabolic
863 adaptation under Cd stress conditions. Front. Plant Sci. 6, 138.
864 https://doi.org/10.3389/fpls.2015.00138.
865 27. Horiunova, I.I., Yemets, A.I. 2015. Effect copper on actin filaments organization in
866 Arabidopsis thaliana root cells. Fakt. Eksp. Evol. Organ. 16, 41-45.
867 28. Horiunova, I.I., Krasylenko, Y.A., Yemets, A.I. Blume, Y. B. 2016. Involvement of plant
868 cytoskeleton in cellular mechanisms of metal toxicity. Cytol. Genet. 50, 47-59.
869 https://doi.org/10.3103/S0095452716010060.
870 29. Ialelou, F.S., Shafagh-Kolvanagh, J., Fateh, M. 2013. Effect of various concentrations of zinc
871 on chlorophyll, starch, soluble sugars and proline in Naked pumpkin (*Cucurbita pepo*). Int. J.
872 Farm. Allied Sci. 24, 1198-1202. http://dx.doi.org/10.12692/ijb/4.10.6-12.
873 30. Jiang, X., Wang, C. 2008. Zinc distribution and zinc-binding forms in *Phragmites australis*
874 under zinc pollution. J. Plant Physiol. 165, 697-704.
875 https://doi.org/10.1016/j.jplph.2007.05.011.
876 31. Kim, S.J., Brandizzi, F. 2014. The plant secretory pathway: an essential factory for building
877 the plant cell wall. Plant Cell Physiol. 55, 687-93. doi: 10.1093/pcp/pct197.
878 32. Klink, A. 2017. A comparison of trace metal bioaccumulation and distribution in *Typha*
879 *latifolia* and *Phragmites australis*: implication for phytoremediation. Environ Sci Pollut Res
880 Int. 24, 3843-3852. doi: 10.1007/s11356-016-8135-6.
881 33. Klink, A., A. Maciol, Wislocka, M., Krawczyk. J. 2013. Metal accumulation and distribution
882 in the ogans of Typha latifolia L. (cattail) and their potential use in bioindication. Limnologica
883 43, 164-168. https://doi.org/10.1016/j.limno.2012.08.012.
884 34. Krzeslowska, M. 2011. The wall cell in plant cell response to trace metals: Polysaccharide
885 remodeling and its role in defense strategy. Acta Physiol. Plant. 33, 35-51.
886 https://doi.org/10.1007/s11738-010-0581-z.

887 35. Kulikova, A.L., Kholodova, V.P., Kuznetsov, V.V. 2009. Actin is involved in early plant
888 responses to heavy metal stress and associates with molecular chaperons in stress
889 environments. Russ. J. Rep. Dev. Biol. Sci. 424, 49-52.
890 https://doi.org/10.1134/S0012496609010153.
891 36. Kumar, S., and Trivedi, P. K. 2016. Heavy metal stress signaling in plants. in Plant Metal
892 Interaction- Emerging Remediation Techniques, ed. P. Ahmad (Amsterdan: Elsevier), 58-603.
893 doi: 10.1016/B978-0-12-803158-2.00025-4.
894 37. Laemmli, U. K. 1970. Cleavage of structural proteins during the assembly of the head of
895 bacteriophage T4. Nature 227, 680-685. https://doi.org/10.1038/227680a0.
896 38. Le Gall, H., Philippe, F., Domon, J.M., Gillet, F., Pelloux, J., Rayon, C. 2015. Cell wall
897 metabolism in response to abiotic stress. Plants, 4, 112-166.
898 https://doi.org/10.3390/plants4010112.
899 39. Li, Y.-Q., Mareck, A., Faleri, C., Moscatelli, A., Liu, Q. Cresti M. 2002 Detection and
900 localization of pectin methyl esterase isoforms in pollen tubes of *Nicotiana tabacum* L. Planta
901 214, 734-740.
902 40. Lingua, G., Bona, E., Todeschini, V., Cattaneo, C., Marsano, F., Berta, G., Cavaletto, M. 2012.
903 Effects of heavy metals and arbuscular mycorrhiza on the leaf proteome of a selected poplar
904 clone: a time course analysis. PLoS One 7: e38662.
905 https://doi.org/10.1371/journal.pone.0038662.
906 41. Liu, T.; Shen, C.; Wang, Y.; Huang, C.; Shi, J. 2014 New insights into regulation of proteome
907 and polysaccharide in cell wall of *Elsholtzia splendens* in response to copper stress. PLoS
908 One, 9, e109573. https://doi.org/10.1371/journal.pone.0109573.
909 42. Liu, Y., Espinosa, C.D., Abelilla, J.J., Casas, G.A., Lagos, L.V., Lee, S.A., Kwon, W.B.,
910 Mathai, J.K., Navarro, D.M.D.L., Jaworski, N.W., Stein, H.H. 2018 Non-antibiotic feed
911 additives in diets for pigs: A review. Anim. Nutr. 4,113-125.
912 https://doi.org/10.1016/j.aninu.2018.01.007.

913 43. Maksymiec W, Bednara J, Baszynski T 1996. Different susceptibility of runner bean plants to
914 excess copper as a function of the growth stages of primary leaves. Journal of Plant Physiology
915 149, 217-221. https://doi.org/10.1016/S0176-1617(96)80198-2.
916 44. Małachowska-Jutsz, A., Gnida, A. 2015. Mechanisms of stress avoidance and tolerance by
917 plants used in phytoremediation of heavy metals. Arch. Env. Prot. 41, 104-114.
918 https://doi.org/10.1515/aep-2015-0045.
919 45. Manios, T., Stentiford, E.I., Millner, P.A., 2003. The effect of heavy metals accumulation on
920 the chlorophyll concentration of *Typha latifolia* plants, growing in a substrate containing
921 sewage sludge compost and watered with metaliferus water. J. Ecolo. Eng. 20, 65-74.
922 https://doi.org/10.1016/S0925-8574(03)00004-1.
923 46. Manna, S. 2015. An overview of pentatricopeptide repeat proteins and their applications.
924 Biochimie 113, 93-99. https://doi.org/10.1016/j.biochi.2015.04.004.
925 47. McManus, H.A., Seago, J.L., Marsh, L.C. 2002. Epifluorescent and histochemical aspects of
926 shoot anatomy of *Typha latifolia* L., *Typha angustifolia* L. and *Typha glauca*, Godr. Ann Bot.
927 90, 489-93. https://doi.org/10.1093/aob/mcf211.
928 48. Meier, S., Alvear, M., Borie, F., Aguilera, P., Ginocchio, R. & Cornejo, P. 2012. Influence of
929 copper on root exudate patterns in some metallophytes and agricultural plants. Ecotoxicology
930 and Environmental Safety, 75, 8-15. https://doi.org/10.1016/j.ecoenv.2011.08.029.
931 49. Molas, J. 2002. Changes of chloroplast ultrastructure and total chlorophyll concentration in
932 cabbage leaves caused by excess of organic Ni(II) complexes. Environ Exp Bot 47, 115-126.
933 https://doi.org/10.1016/S0098-8472(01)00116-2.
934 50. Nicholson, F.A., Smith, S.R., Allowayc, B.J., Carlton-Smithd, C., Chambersa, B.J. 2003. An
935 inventory of heavy metals inputs to agricultural soils in England and Wales. Sci Total
936 Environ., 311, 205-219. https://doi.org/10.1016/S0048-9697(03)00139-6.

937 51. Nyitrai, P., Bóka, K., Gáspár, L., Sárvári, E., Keresztes, A. 2004. Rejuvenation of ageing bean
938 leaves under the effect of low-dose stressors. Plant Biol. 6, 708-714. doi:10.1055/s-2004-
939 830385.
940 52. Onelli, E., Idilli, A.I., Moscatelli, A. 2015. Emerging role for microtubules in angiosperm
941 pollen tube growth highlight new research cues. Front Plant Sci. 10, 51. doi:
942 10.3389/fpls.2015.00051.
943 53. Oves, M., Saghir Khan, M, Huda Qari, A., Nadeen Felemban, M., Almeelbi, T. 2016. Heavy
944 metals: biological importance and detoxification strategies. J Bioremed Biodeg 7, 334.
945 http://dx.doi.org/10.4172/2155-6199.1000334.
946 54. Peterson, H G. 1998 Use of constructed wetlands to process agricultural wastewater. Can. J.
947 Plant Sci. 78, 199-210. https://doi.org/10.4141/P97-142.
948 55. Petraglia, A., De Benedictis, M., Degola, F., Pastore, G., Calcagno, M., Ruotolo, R., Mengoni,
949 A. Sanità di Toppi, L. 2014 The capability to synthesize phytochelatins and the presence of
950 constitutive and functional phytochelatin synthases are ancestral (plesiomorphic) characters
951 for basal land plants. J Exp Bot. 65, 1153-1163. http://dx.doi.org/10.1093/jxb/ert472.
952 56. Rao, K.P., Vani, G., Kumar, K., Wankhede, D.P., Misra, M., Gupta, M., Sinha, A.K. 2011.
953 Arsenic stress activates MAP kinase in rice roots and leaves. Arch. Biochem. Biophys. 506,
954 73–82. http://dx.doi.org/10.1016/j.abb.2010.11.006.
955 57. Rufner, R., Barker, A.V., 1984. Ultrastructure of zinc induced iron deficiency in mesophyll
956 chloroplasts of spinach and tomato. J. Am. Soc. Hortic. Sci. 109, 164–168.
957 58. Sandalio, L.M., Dalura, H.C., Gomez, M., Romero-Puertas, M.C., Rio, L.A. 2001. Cadmium
958 induced changes in the growth and oxidative metabolism of pea plants. J. Exp. Bot. 52, 2115-
959 2126. http://dx.doi.org/10.1093/jexbot/52.364.2115.
960 59. Singh, S., Parihar, P., Singh, R., Singh, V. P., and Prasad, S. M. 2016. Heavy metal tolerance
961 in plants: role of transcriptomics, proteomics, metabolomics, and ionomics. Front. Plant Sci.
962 6, 1143. http://dx.doi.org/10.3389/fpls.2015.01143.

963 60. Sinha, P., Poland, J., Schnolzer, M., Rabilloud, T. 2001. A new silver staining apparatus and
964 procedure for matrix-assisted laser desorption/ ionization-time of flight analysis of proteins
965 after two-dimensional electrophoresis. Proteomics 1, 835-840.
966 http://dx.doi.org/10.1002/1615-9861
967 61. Soskic, V., Go¨rlach, M., Poznanovic, S., Boehmer, F. D. and Godovac Zimmermann, J. 1999.
968 Functional proteomics analysis of signal transduction pathways of the platelet-derived growth
969 factor beta receptor. Biochemistry 38, 1757-1764. https://doi.org/10.1021/bi982093r.
970 62. Stoláriková-Vaculíková, M., Romeo, S., Minnocci, A., Luxová, M., Vaculík, M., Lux, A.,
971 Sebastiani, L. 2015. Anatomical, biochemical and morphological responses of poplar *Populus*
972 *deltoides* clone Lux to Zn excess. Environ. Exp. Bot. 109, 235-243.
973 https://doi.org/10.1016/j.envexpbot.2014.07.001.
974 63. Tian, H., Baxter, I.R., Lahner, B., Reinders, A., Salt, D.E., Ward, J.M. 2010. Arabidopsis
975 NPCC6/NaKR1 is a phloem mobile metal binding protein necessary for phloem function and
976 root meristem maintenance. Plant Cell 22, 3963-3979.
977 https://doi.org/10.1105/tpc.110.080010.
978 64. Tiwari, S., Lata, C. 2018. Heavy Metal stress, signaling, and tolerance due to plant-associated
979 microbes: an overview. Front. Plant Sci. 9, 452. https://doi.org/10.3389/fpls.2018.00452.
980 65. Todeschini, V., Lingua, G., D'Agostino, G., Carniato, F., Roccotiello, E., Berta G. 2011.
981 Effects of high zinc concentration on poplar leaves: a morphological and biochemical study.
982 Environ. Exp. Bot., 71, 50-56. https://doi.org/10.1016/j.envexpbot.2010.10.018.
983 66. Viehweger, K. 2014. How plants cope with heavy metals. Botanical Studies. 55, 35
984 https://doi.org//10.1186/1999-3110-55-35.
985 67. Yadav, S.K. 2010. Heavy metals toxicity in plants: An overview on the role of glutathione
986 and phytochelatins in heavy metal stress tolerance of plants. South Afr. J. Bot. 76, 167-179.
987 https://doi.org/10.1016/j.sajb.2009.10.007.

68. Yang, J., Ye, Z. 2009. Metal accumulation and tolerance in wetland plants. Front. Biol. China. 4, 282-288. https://doi.org/10.1007/s11515-009-0024-7.

69. Yang, Y.Y., Jung, J.Y., Song, W.Y., Suh, H.S., Lee, Y. 2000. Identification of rice varieties with high tolerance or sensitivity to lead and characterization of the mechanism of tolerance. Plant Physiol. 124, 1019-1026. https://doi.org/10.1104/pp.124.3.1019.

70. Zappala, M.N., Ellzey, J.T., Bader, J., Peralta-Videa, J.R., Gardea-Torresdey, J. 2014. Effects of copper sulfate on seedlings of *Prosopis pubescens* (screwbean mesquite). Int. J. Phytoremed. 16, 1031-1041. https://doi.org/10.1080/15226514.2013.810582.